

Modelling experimental uveitis: barrier effects in autoimmune disease

David Nicholson · Emma C. Kerr · Owen G. Jepps ·
Lindsay B. Nicholson

Received: 10 November 2011/Revised: 10 February 2012/Accepted: 16 March 2012/Published online: 10 April 2012
© Springer Basel AG 2012

Abstract

Objective and design A mathematical analysis of leukocytes accumulating in experimental autoimmune uveitis (EAU), using ordinary differential equations (ODEs) and incorporating a barrier to cell traffic.

Materials and subjects Data from an analysis of the kinetics of cell accumulation within the eye during EAU.

Methods We applied a well-established mathematical approach that uses ODEs to describe the behaviour of cells on both sides of the blood–retinal barrier and compared data from the mathematical model with experimental data from animals with EAU.

Results The presence of the barrier is critical to the ability of the model to qualitatively reproduce the experimental data. However, barrier breakdown is not sufficient to produce a surge of cells into the eye, which depends also on asymmetry in the rates at which cells can penetrate the

barrier. Antigen-presenting cell (APC) generation also plays a critical role and we can derive from the model the ratio for APC production under inflammatory conditions relative to production in the resting state, which has a value that agrees closely with that found by experiment.

Conclusions Asymmetric trafficking and the dynamics of APC production play an important role in the dynamics of cell accumulation in EAU.

Keywords Mathematical modelling · Autoimmunity · Barrier permeability · Blood–retinal barrier

Introduction

Accumulation of leukocytes in the target organ is a hallmark of autoimmunity. This process is widely believed to be co-ordinated by specific CD4⁺ T lymphocytes responding to locally presented antigen [1]. In many situations, this accumulation requires that cells pass through basement membranes, such as those associated with the blood–brain barrier and the blood–retinal barrier (BRB), that limit macromolecular and cellular entry [2]. Alterations in barrier permeability are therefore key to the disease process.

We have studied immune cell entry into the eye in the murine model of inflammatory eye disease, experimental autoimmune uveoretinitis (EAU). Experiments have shown that, during early disease (before day 30), cell trafficking is a highly dynamic process [3]. Enumerating CD4⁺ and CD11b⁺ cells in the target organ reveals rapid changes in ocular cell content which oscillate with time. Furthermore, treatment of animals that have ocular inflammation with FTY720, a drug that arrests the recirculation of CD4⁺ cells, provokes a rapid exodus of leukocytes from the eye [4],

Responsible Editor: Graham Wallace.

D. Nicholson · E. C. Kerr · L. B. Nicholson
School of Cellular and Molecular Medicine, Medical Sciences
Building, University of Bristol, University Walk,
Bristol BS8 1TD, UK

O. G. Jepps
Queensland Micro- and Nanotechnology Centre, School
of Biomolecular and Physical Sciences, Griffith University,
Brisbane, QLD 4111, Australia

L. B. Nicholson
Academic Unit of Ophthalmology, School of Clinical Sciences,
University of Bristol, Bristol Eye Hospital, Bristol BS1 2LX, UK

L. B. Nicholson (✉)
F44, Medical Sciences Building, University Walk,
Bristol BS8 1TD, UK
e-mail: l.nicholson@bristol.ac.uk

providing a direct demonstration that at the peak of disease cells can move rapidly from one side of the BRB to the other.

Monitoring clinical disease allows serial analysis of individual eyes in EAU. While not as sensitive a measure of variation in the level of infiltration as counting cells, it does confirm, in many individual eyes, an underlying fluctuating disease course (J. Boldison and L. Nicholson, unpublished data). Shao and co-workers [5] reported results in the Lewis rat EAU model, obtained by clinical scoring, that also exhibited similar oscillatory behaviour; however, this report did not distinguish changes in individual cell populations. Observations such as these are not restricted to EAU and quantitative experiments in other autoimmune diseases have also revealed rapid changes in specific immune cell number. In non-obese diabetic mice, staining CD8⁺ cells from peripheral blood with tetramers that detected cells capable of recognising an autoantigen showed oscillations in cell number as disease developed [6].

These considerations have led us to formulate a mathematical model to probe the role that changes in BRB barrier function might play in determining the dynamics of cell trafficking into and out of the eye, since, to the best of our knowledge, models of the immune system that attempt to include barrier effects have not previously been investigated mathematically. There is already a wealth of information regarding the molecular mechanisms that regulate the accumulation of leukocytes at sites of inflammation [7–9]. Much less has been made of the importance of the dynamics of T-cell generation, antigen-presenting cell (APC) mobilisation and the role of the barrier in determining the course of disease. Our aim here is to establish a model that contains a minimal number of dynamical equations consistent with the biologically understood behaviour of the immune response as manifested in EAU. We chose to approach the modelling of the experimental data by using the assumption that the relative concentrations of cells on either side of the barrier are a function of cell number and the presence of a barrier that may promote or impede cell exchange. In this regard, our system is a natural extension to a well-established class of single-compartment population models that have been proposed and used to analyse the dynamics of the immune response [10–13].

Through the incorporation of the barrier and by choosing parameters close to values deduced from experimental data (where these are available), our model can qualitatively reproduce the main features observed experimentally whilst the equivalent model without a barrier fails to do so. Furthermore, this study reveals two novel biological insights: first, that global barrier disruption alone cannot lead to a surge of cells into the eye comparable to that

observed experimentally, and second that the dynamics of APC generation and recruitment are critical parameters, with a significant impact on the behaviour of the system. Finally, by solving the equations using estimated values for APC turnover and murine eye volume, we derive a value for the maximum increase in APC production under inflammatory conditions that agrees closely with that found by experiment.

Results

Outline of the model

The model (Fig. 1) consists of a set of ordinary differential equations (see “Appendix”) that describe the dynamics of autoantigen-specific T-cell (T) and APC (A) populations inside and outside the eye. These populations are subdivided on the basis of their location (denoted by subscripts), their activation state (the activated state being denoted by a superscript asterisk) and their history. The model is simplified in that we consider only one type of T cell and one type of APC, counted in each of the two compartments which are separated by a variably permeable barrier. The behaviour of the system is then expressed in terms of the customary mass action equations, where it is assumed that concentrations are uniform within each compartment. This means that any movement across the BRB depends on the relative concentrations of cells in each compartment, but an important distinction from single compartment models is that different uniform concentrations can exist on either side of the BRB. The global properties of the barrier are subject to modification during the course of disease and the rate of permeation of different cell types through the barrier is controlled by permeability constants K that the model allows to change asymmetrically.

Certain features of the way the model represents what is known about the ocular autoimmune response are worth emphasising. ‘Activation’ of APCs and T cells is conceived to represent two different immunological processes. For the APCs, activation denotes the acquisition of epitopes and appropriate costimulatory molecules which confer on these cells the potential to stimulate autopathogenic T cells. The epitopes can be acquired either as a result of ‘immunisation’, in which case the resulting APCs are only found outside the eye (A_{oo}^*), or they can be acquired within the eye. This acquisition depends on the presence of activated T cells within the eye (T_i^*), which are necessary to produce A_i^* cells (Fig. 1). T-cell activation is only considered for those cells with T-cell receptors that can recognise ocular antigens and occurs when an activated APC encounters such a T cell. The model does not enumerate other T cells. In the periphery, the interaction of activated T and A cells

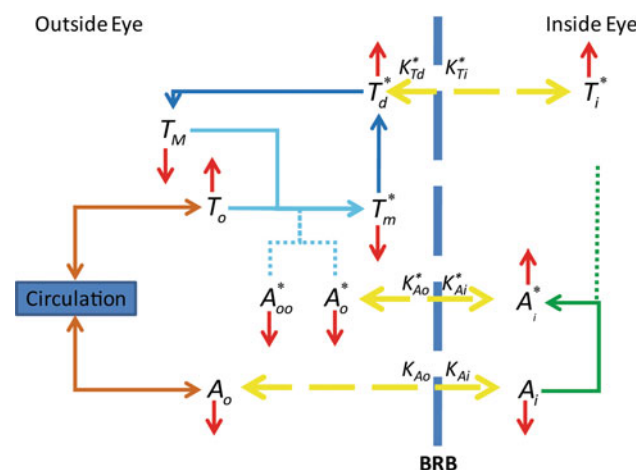


Fig. 1 Two-compartment model of EAU. The model comprises two compartments separated by the blood–retinal barrier (BRB). Two types of cell are counted, T cells and A cells. These can be in different places, outside the eye (T_o/A_o) or inside the eye (T_i/A_i), and in a number of different states [e.g. activated ($*$) or unactivated]. Activated A cells (A^*) drive the activation of T cells outside the eye (dotted blue line) and activated T (T^*) cells drive the activation of A cells within the eye (dotted green line). Cells move between the two compartments by crossing the BRB. Some cells can change state (solid arrows) and all cells can die (red arrows) (color figure online)

stimulates antigen-specific population growth, shown for ease of mathematical manipulation as the production of activated daughter cells (T_d^*) from mother cells (T_m^*). These daughter cells may die or may become memory cells (T_M). One important feature of our model is that T cells do not divide within the eye. This aspect is based on our extensive experimental work, which shows that the ocular microenvironment limits T-cell proliferation [3, 14, 15].

Since the model counts only autoantigen-specific T cells, it implicitly assumes that non-specific T cells play no significant role in the dynamics we are modelling. All cells have the potential to die (indicated by the red arrows in Fig. 1). The model moves forward through time and unactivated T and A cells arise continuously de novo. In animals these cells come originally from bone marrow stem cells, followed, in the case of the T cells, by selection in the thymus. These events are handled, following the work of others, as logistic equations [16, 17] that incorporate as a parameter a maximum carrying capacity for each cell type.

An important consideration of the model is the physical size of the eye. Experimentally, our analyses of the mouse eye yield total cell counts, but the use of mass action equations to describe concentration-driven permeation across compartments of different volumes necessitates converting these numbers to concentrations. We can establish reasonable parameters for retinal volumes from direct measurement (H. Xu, University of Belfast, personal communication) but the volume outside the eye from

which cells can move into the eye is more difficult to estimate. We conceptualise this as the available vascular volume within the retina from which cells can be exchanged. As discussed below, this exchange volume is constrained by the model.

Modelling

The parameter space of our model is many-dimensional, rendering a general exploration unfeasible. The model was therefore analysed to yield limiting values with specific parameters (see below) and the equations (see “Appendix”) were solved numerically, using Taylor expansion. There are various schemes available for solving differential equations numerically, with differing strengths and weaknesses. We have chosen a scheme that uses a third-order Taylor series approximation to the solution. The first-, second- and third-order derivatives of the variables are used in our system to compute the values of these variables at fixed intervals Δt . These higher order derivatives are established directly from the first-order derivatives given in Eqs. (1)–(10), using the chain and product rules. The time step Δt was adjusted to ensure that the error terms were negligible throughout the simulation. This approach requires more calculation than lower-order methods, but the advantage is higher accuracy in the solution. For the calculations, we adopted the values for parameters as given in Table 1. The species described and their doubling times and half-lives are detailed in Tables 2 and 3. For many of these, we were able to ascribe reasonable values from the literature (see “Appendix”).

Experimental data

The data we use are based on experiments carried out in B10.RIII mice and reported elsewhere [3]. Briefly, EAU was induced by immunisation with peptide and adjuvants in a large number of animals which were killed at various time points. Eyes were collected and $CD4^+$ and $CD11b^+$ cells were enumerated in tissue including the retina and the ciliary marginal zone but not the choroid or iris (Fig. 2). The number of cells per eye was calculated as a mean value from all the eyes acquired on any particular day and each data point represents the average of 4–8 separate measurements. To convert cell numbers to concentrations, the cell counts have been converted to a number concentration (number of cells cm^{-3}) based on a value for the retinal volume of $2.29 (\pm 0.2) \times 10^{-3} cm^3$. From these data we defined a number of characteristic criteria that we could compare with results predicted by the model. These are time and concentration of the first maximum, the period of the first oscillation, the ratio of concentration of the first

Table 1 Parameter set for basic calculations

Parameter	Description	Value	Ref
a	Rate of production of T or A cells	$a_T = 8 \times 10^{-2} \text{ cm}^{-3} \text{ day}^{-1}$; $a_A = \text{calculated from Eq. (22)}$	[38]
α_T and α_A	Activation rate of T and A cells	$2.0 \times 10^{-4} \text{ cm}^3 \text{ day}^{-1}$	[30]
β	Differentiation of activated (effector) daughter cells to memory cells	$8.66 \times 10^{-4} \text{ h}^{-1}$	[48]
δ	Death rate derived from the following half-lives in days	$T_o = 57, T^* = 6, A = 3, A^* = 3$	[30, 38, 40]
K	Permeability constants	$1.00 \times 10^{-4} \text{ h}^{-1}$ to $2.50 \times 10^{-4} \text{ h}^{-1}$	[49]
v	Ratio of the volume occupied by populations within the retina to the volume occupied by populations in the peripheral volume	61.9	H. Xu, personal communication
p	Division rate (proliferation) of cells, based on the following doubling time in hours	$A = 17, T = 24, T^* = 8$	[30, 35, 36, 50]
T_d d	Onset of primary proliferation	10 days	[3]
t_D d	Characteristic time for barrier change	10 days	[31]
T_D d	Onset of differentiation	10 days	[3]
ϕ	Amplification of permeability on barrier breakdown	500	[18]
θ	Ratio A_L/A_o^c	1.26–1.31	Eq. (21)
σ	Maximum amplification effect of activated T cells on BRB	1,000	[18]
μ	Midpoint concentration of the amplification function	$1,000 \text{ cm}^{-3}$	[18]
$H_1(t), H_2(t)$	Heaviside switching function	0, 1	[12]
$h(t)$	Permeation rate		Eq. (12)
T_L, T_{dL}, T_{ML} and A_L	Limiting concentrations in the rate of production terms for the respective species	See “Appendix”	[16, 17]

Table 2 Species and initial concentrations

Cell species	Concentration at time t	Initial concentration (cm^{-3})
Naïve T cells outside ^a the eye	T_o	5.0
Activated (effector) mother T cells outside the eye	T_m^*	0
Activated (effector) daughter T cells outside the eye	T_d^*	0
Memory cells outside the eye	T_M	0
Activated (effector) T cells inside the eye	T_i^*	0
Non-activated APCs outside ^a the eye	A_o	5.0×10^5
Non-activated APCs inside ^b the eye	A_i	2.9×10^5
Activated APCs outside the eye	A_i^o	0
Activated APCs inside the eye	A_i^*	0
Activated AP cells outside ^a the eye from immunisation	A_{oo}^*	1×10^3

^a The external concentrations are mean values for the whole system, assumed to be valid within the vascular volume

^b This is the concentration inside the retina; however not all of these APCs belong to the exchangeable pool of cells, so the A_i concentration may, in effect, be lower than this

Table 3 Doubling times and half-lives

Doubling time		Half-life	
Species	Time (h)	Species	Time (days)
T_o	24	T_o	57
T_d^*, T_m^*	8	T_d^*, T_m^*	6
A	17	A and A^*	3
$T_d^* \rightarrow T_M$	800		

and second peak and the ratio of APCs to T cells within the eye at the second maximum.

Model constants and parameters

Figure 1 shows that the model comprises 10 individual cell states, five for APCs and five for T cells. The change in concentration of each of these is defined by an ordinary differential equation and the mathematical treatment of the

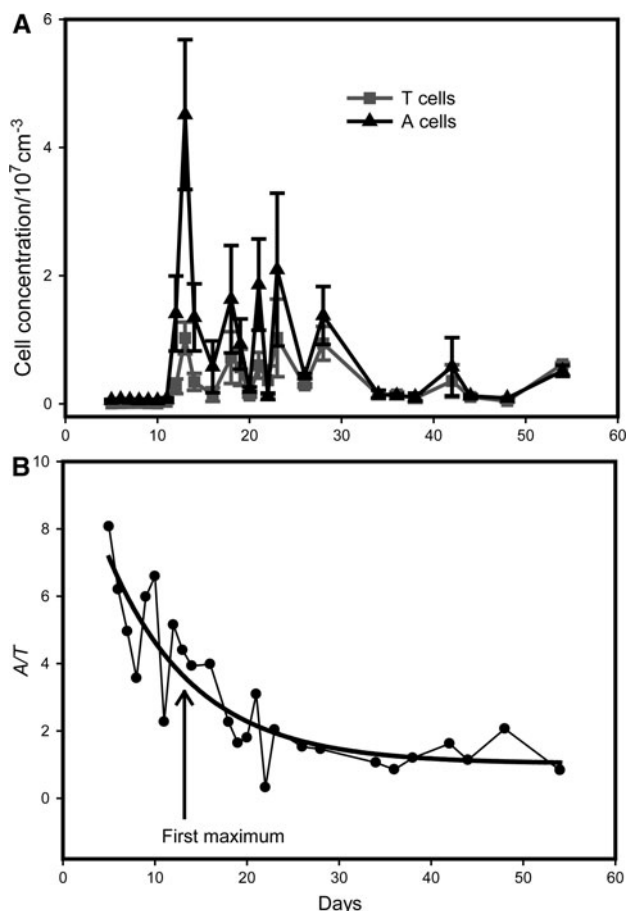


Fig. 2 Experimental data. **a** The concentration of CD4 T⁺ cells and CD11b⁺ antigen presenting cells (APCs) inside the eye calculated based on published data [3] as a function of time; A cells (CD11b⁺ APCs) are shown as triangles and T cells (CD4⁺ cells) as squares. **b** The ratio of APC to T-cell concentration; the heavy line is the best fit exponential decay through the data

model is given in the Appendix. Here we focus on the insights we derive from the model. For many parameters, such as half-life and death-rate constants, it is possible to acquire values from independent experimental data, while for others, for example permeability constants, estimates from experiment are subject to a wide margin of uncertainty. The parameter set chosen for the basic calculation is given in Table 1 and further details on parameter selection are given in the Appendix.

Modification of the BRB by activated T cells

Movement across the BRB is a complex process regulated by many influences, particularly the upregulation of adhesion molecules and their receptors, the activating effects of cytokines and the chemotactic influence of chemokines [7]. In the model, these considerations are addressed indirectly by using cell-specific concentration-

independent permeabilities which are expressed using permeability constants (*K*) to reflect changes in the trafficking properties of individual cell types and global functions that reflect the rapid changes in permeability that occur at barrier breakdown and affect all cells. The permeation rate through the barrier is assumed to be proportional to the concentrations on either side of the barrier. Consistent with experimental data, the unperturbed barrier is permeable to activated cells, which allows the accumulation of T_i^* up to a saturation limit [18]. To model how this accumulation impacts the BRB, we introduced two functions. The first addresses the observation that the barrier breaks down about 10 days after immunisation [3, 19]. To model this, we introduce a sigmoid function with a maximum rate of change that depends on the characteristic time for barrier change t_D . The second increases barrier permeability by a factor varying from unity to a maximum σ as the concentration of T cells within the eye increases. This reflects the influence that a build-up of activated T cells within the eye has on the barrier.

Equilibrium and barrier-free conditions

At equilibrium (indicated by superscript ‘e’), and in the absence of immune system activation, the model retains three species of cell, T cells outside the eye (T_o^e), APCs outside the eye (A_o^e) and APCs within the eye (A_i^e). All other concentrations are zero and the remaining equations can be solved analytically and return a constant value of T_o^e with time. For the T cells, maintenance of homeostasis according to the logistic equation imposes an upper bound on the rate of cell production.

The steady-state values of the APCs are subject to specific limiting values. If the permeability constants are set to be the same in both directions, the equations show that $A_o^e > A_i^e$, as supported by experiment [see Eq. (19) in Appendix]. Analysis of the relationship between the APC concentration at the carrying capacity A_L and their concentration at equilibrium A_o^e reveals that the ratio A_L/A_o^e (defined as θ) has upper and lower bounds that can be expressed in terms of the rates of production and death of APC cells and the ratio of retinal to vascular volumes. For the parameters analysed here, this upper limit for θ is 1.313. Furthermore, for oscillations to occur in the production of APCs the concentration A_o must be close to its limiting value A_L (see Appendix).

To test whether the presence of a barrier changed the behaviour of the system, we analysed a single-compartment model by summing the pairs of Eqs. (4) + (5), (6) + (7) and (8) + (9). This creates a situation in which there is no distinction between external and internal species, although mother, daughter, memory and naïve T cells remain distinct. Using parameters that are identical to those

producing oscillations in the full model, this single compartment model exhibits entirely different behaviour (Fig. 3). The final cell concentrations are not the same and the system does not oscillate as it does in the corresponding two-compartment model. This confirms that in this model the presence of a barrier profoundly influences the behaviour of the system. We proceeded to explore the effects of parameter modification and the extent to which the model can mimic the characteristic behaviour observed in our experiments [3].

Barrier breakdown plays a limited role in regulating cell trafficking

Based on the experimental data, we targeted solutions that give damped oscillations after a delay of about 12 days. We defined five characteristic criteria of the experimental

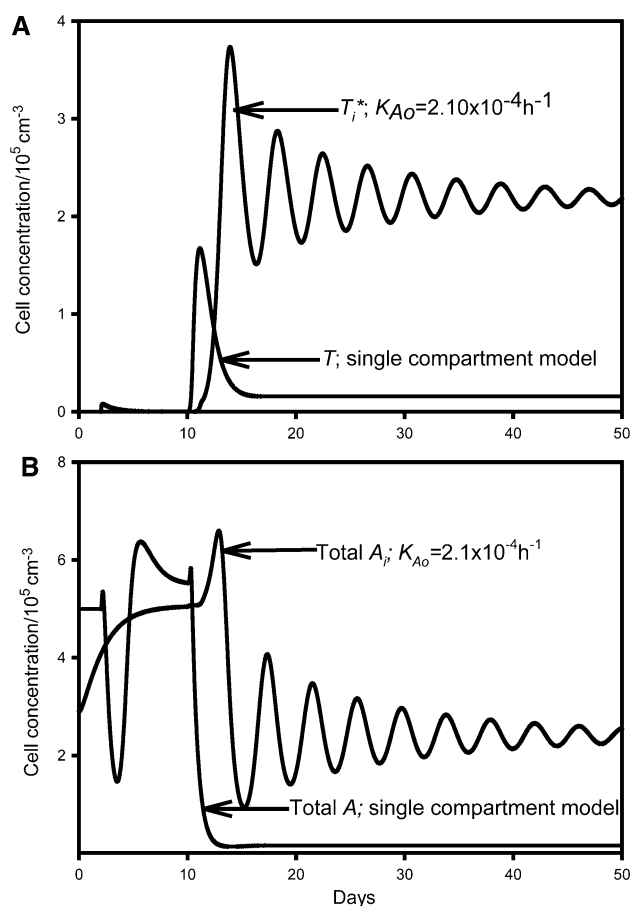


Fig. 3 Comparison of single- and two-compartment models. Data were obtained from the two-compartment model and the same model with the barrier removed by combining Eqs. (1), (2), (3) and (10) with (26), (27) and (28). **a** Comparison of the values found for the concentration of T cells in the eye in the two-compartment model (T_i^*) with total T cells in the single-compartment model (T). **b** Comparison of the concentration of all A cells within the eye ($Total A_i$) with all A cells in the single-compartment model ($Total A$)

data and sought conditions for which the results from the model best approached these values (Table 4). Having established that the barrier plays a role in determining the behaviour of the system, and because of the large body of literature implicating breakdown in the barrier as a key step in uveitis [2, 20, 21], we first examined the effects of global barrier modification. To mimic a disruption in the barrier, leading to a large increase in permeability, we introduced the sigmoid function $h(t)$ [Eq. (12)] discussed earlier. This allowed us to test the impact of changing the permeability of the barrier by a factor of ϕ over a few hours. Over a range of ϕ from 2 to 500, low values of ϕ were associated with stronger damping but changes in this value produced only minor modification in the height and positions of the maxima (Fig. 4a). This shows that, although some alteration in the permeability of the barrier is required for the model to conform to our characteristic criteria, the magnitude of this is not crucial.

The concentration of activated T cells within the eye also has an impact on barrier function. The parameter σ represents the maximum increase in traffic that the presence of these cells can induce and values are based on the changes that the administration of tumour necrosis factor- α has on the rate of neutrophil traffic across endothelium. A reasonable estimate of the magnitude of this effect taken from the literature is $\sigma = 1,000$ and using this value in the model results in damped oscillations [18]. Although this is a numerically large effect, we find that the behaviour of the model is very insensitive to changes in this parameter—reducing σ by two orders of magnitude resulted in only a small change in damping (Fig. 4b). Only if the effects of activated T cells on the barrier are removed completely by setting $\sigma = 1$ is there much impact, in that the oscillations are much more strongly damped and have a longer period. These results show that although barrier disruption does modify the observed behaviour, including the threshold for oscillation, and the existence, magnitude and damping of the oscillations, the response is relatively insensitive to the values of parameters that define the size of this effect. Therefore, based on the present model, barrier breakdown in its simplest form cannot be wholly responsible for the experimental observations.

Control of the model by permeability and APC parameters

Since simple disruption is not sufficient to reproduce the experimental findings, we examined the effects of modifying other aspects of barrier function. Traffic across the barrier by the different cell types is also determined by the permeability constants K . The model allows us to assign individual permeability constants to each cell species that crosses that barrier. The equations for the equilibrium state

Table 4 Characteristic criteria from experiment and theory

	First maximum						
	Run	K_{A_0} (10^{-4} h^{-1})	Day	Conc (10^5 cm^{-3})	1st to 2nd period	Conc 1st/Conc 2nd	$(A_i^* + A_i)/T^*$ at 2nd maximum
$\theta = 1.260$	1	1.00	10.5	30.0	No oscillation		
$\theta/\theta_{\max} = 0.9571$	2	1.30	11.3	11.7	5.7	4.5	1.0
	3	1.60	12.1	8.6	4.6	3.1	1.1
	4	1.90	12.6	7.3	4.4	2.4	1.2
	5	2.20	13.1	6.6	4.4	2.1	1.2
	6	2.50	13.5	6.2	4.4	1.9	1.2
$\theta = 1.290$	7	1.00	10.5	31.0	No oscillation		
$\theta/\theta_{\max} = 0.9826$	8	1.30	11.4	11.4	5.0	5.7	1.2
	9	1.60	12.1	8.4	4.5	2.9	1.5
	10	1.90	12.6	7.2	4.4	2.1	1.6
	11	2.20	13.1	6.5	4.3	1.8	1.6
	12	2.50	13.4	6.0	4.4	1.7	1.6
$\theta = 1.300$	13	1.00	10.6	37.1	No oscillation		
$\theta/\theta_{\max} = 0.9902$	14	1.30	11.3	11.3	5.0	4.9	1.6
	15	1.60	12.1	8.5	4.6	2.4	2.0
	16	1.90	12.5	7.1	4.5	1.8	2.0
	17	2.20	13.1	6.4	4.4	1.6	2.1
	18	2.50	13.4	5.9	4.5	1.5	1.9
$\theta = 1.310$	19	1.00	10.6	31.0	7.1	47.0	1.3
$\theta/\theta_{\max} = 0.9978$	20	1.10	10.9	18.0	5.9	8.6	2.4
	21	1.30	11.5	11.3	5.0	2.5	3.8
	22	1.60	12.1	8.2	4.8	2.2	4.0
	23	1.90	12.6	7.0	4.8	1.32	4.0
	24	2.20	13.0	6.3	4.8	1.23	3.7
	25	2.50	13.4	5.9	4.7	1.25	2.8
Experiment	–		13.2	428	4.9	2.6	2.9

Characteristic criteria were calculated for a range of values of K_{A_0} and are displayed in comparison with the values found by experiment. *Conc* concentration

show that the equilibrium concentrations of APC inside and outside the retina are not equal if the barrier permeability is the same in each direction. To simplify the investigation of the model, we then used separate values for cells moving into the eye (K_o) and for cells moving out (K_i) for all species. Preliminary calculations showed that the system is highly sensitive to the magnitude of these permeability constants.

If we choose a single permeability constant: $K_A = K_{A_0} = K_{A_i}$, then Eq. (21) shows that $A_o^c > A_i^c$, as supported by experimental observation. When both outgoing and ingoing permeabilities are set to be identical, then using our defined set of parameters, we find $K_{A_0} = 2.14 \times 10^{-4} \text{ h}^{-1}$. If the barrier permeability is asymmetric, K_{A_i} can be calculated from the equilibrium condition in Eq. (21) of the Appendix and a value of K_{A_0} between the upper and lower limits imposed by this equation found (see “Appendix” for detail). Trial calculations with values with $K > 2.6 \times 10^{-4} \text{ h}^{-1}$ could not be

completed because concentrations rapidly diverge and when K_{A_0} approaches its minimum value, K_{A_i} approaches zero. This would mean that no cells could permeate out of the eye and very high concentrations of APCs would accumulate within the eye. However, out of a wide-ranging search of the parameters, we found no instances of oscillations at this limit.

With values of K_{A_0} between 1.0 and $2.5 \times 10^{-4} \text{ h}^{-1}$ the model exhibits oscillatory behaviour with characteristic values that approach the experimental data, with the notable exception of the high first maximum concentration (Table 4), which exceeds any value predicted by the model by at least an order of magnitude. As can be seen from Table 4, the position of the maximum is quite responsive to variation of the θ and K_{A_0} parameters. When extremely high maxima, commensurate with experiment, are achieved by increasing K_{A_0} with the consequence that K_{A_i} approaches zero, these initial stages resemble experiment more closely.

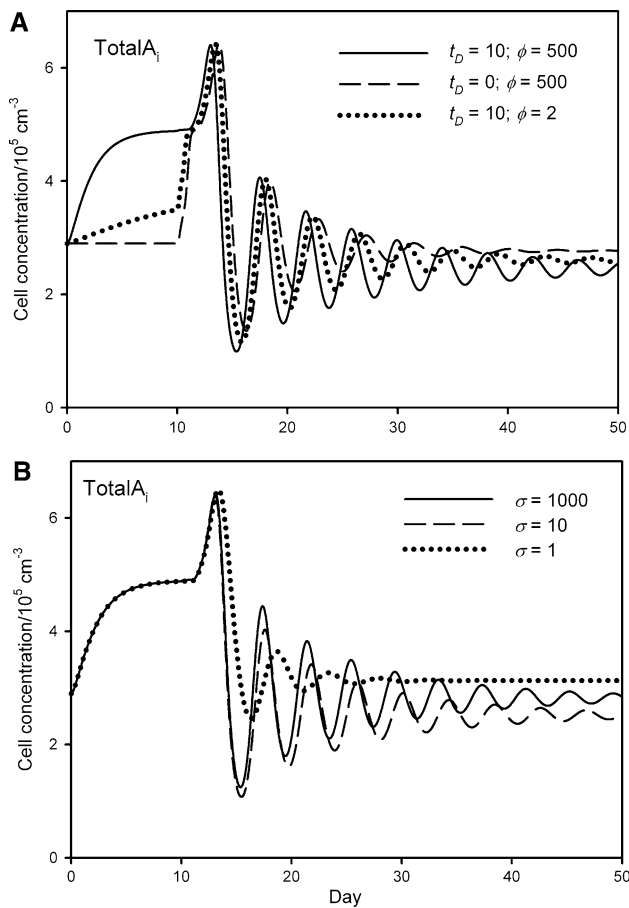


Fig. 4 Effect of changing the global properties of the barrier. **a** The magnitude of the increase in barrier permeability when it breaks down has little effect on the behaviour of the system. Comparison of the concentration of Total A_i when barrier permeability undergoes a two-fold increase ($\phi = 2$) with a 500-fold increase ($\phi = 500$). **b** T-cell activation of the barrier has a small effect across a wide range of values. When activated T cells have no effect on the barrier ($\sigma = 1$) the resulting oscillation in Total A_i is heavily damped, but for values $10 < \sigma < 1,000$ there is only a very small change in Total A_i numbers or in the frequency of oscillation

Further analysis also revealed the unexpected importance of the dynamics of APC production. In the resting state, it is possible to define the maximum value of the parameter θ in terms of the ratio of the concentration of APCs outside the eye at equilibrium to the maximum concentration of APCs that can be achieved. We can also calculate θ in terms of the relative concentrations of APCs within and outside the eye, the rate that these cells die and the rate that they are produced from the bone marrow. The model can then be interrogated in terms of the ratio of θ/θ_{\max} . Calculations show that θ has to be very close to its maximum value for oscillations to occur in the production of APCs; that is, the concentration A_o must be close to its maximal value A_L (Appendix). It follows from this that oscillations are a feature of the rate of APC output approaching its maximum value.

Using the parameters tested here, we found the maximum value of θ to be 1.313. Independent corroboration for this value comes from studies performed in the 1970s that determined rates of the production and kinetics of mononuclear phagocyte accumulation under resting or inflammatory conditions [22]. These experiments were carried out over a much shorter time scale than EAU, and studied trafficking into the peritoneal cavity, nevertheless measurement by two different methods yielded values for the ratio of the maximum concentration of monocytes to the steady state concentration of these cells in the range 1.12–1.63, in good agreement with the value (1.313) we find by calculation.

Discussion

The accumulation of leukocytes in response to stranger and danger signals [23] is a fundamental feature of inflammation. In ocular autoimmunity it is particularly striking, because of the very low numbers of resident immune cells and their rapid concentration within the eye during the course of inflammatory disease. This accumulation is accompanied by dramatic changes in the properties of the BRB and a large number of interactions have been shown to impact on this process. The perception that a breakdown in the barrier is critical to this fundamental process motivated our construction of a simplified model. Here we have used a set of ordinary differential equations to define changes in cell concentrations in different compartments and have included, as a novel feature, terms that allowed us to reproduce rapid alterations in the barrier properties. To assess the model we have made use of quantitative data obtained from animals with experimental autoimmune uveitis, from which we have derived a number of characteristic criteria. The model was tested against its match with the experimental data over a range of different parameters.

We show in this study that the presence of the barrier has a profound impact on the dynamics of the system. If the barrier is removed while keeping all relevant parameters constant (Fig. 3), the oscillations are abolished and there are marked changes in the steady-state concentrations of T cells and APCs at the end of the simulation (equivalent to 50 days). With the barrier present, we could achieve a more accurate representation of the experimental data but, surprisingly, the behaviour of the model was found to be relatively insensitive to the extent to which the barrier impeded the trafficking of cells. An effectively impermeable barrier did not produce a realistic representation of the experimental data, but once traffic through the barrier was possible, global changes over at least two orders of magnitude had little impact on the behaviour of the model. One

reason for this is that points of equilibrium are only weakly dependent on the rate at which cells can move from one side of the barrier to the other, but it is this feature that is most affected by ‘opening up’ the BRB.

Experimentally, measuring cell numbers at a single time point cannot distinguish between many different cells trafficking rapidly through the eye or a few cells with long dwell times that only move in and out of the eye slowly. However, by repeated sampling we find fast accumulation of cells leading to the primary peak of disease [3] and by arresting cell movement, using treatment with fingolimod [4], we have shown a dramatic exodus of cells from the eye. Both of these experiments indicate that in the presence of pathological inflammation, cell turnover in the target organ can be very rapid.

A further important consideration arising from this work is that while we have modelled changes in permeability as arising from alterations in barrier function, an alternative but valid approach would be to conceptualise this in terms of changes in the expression patterns of surface molecules on the cells that govern the rates of trafficking into and out of the eye. While the mathematical modelling of this would be essentially the same, the biological and therapeutic implications might be different and these are therefore important considerations for further experimental exploration.

The model system was sensitive to changes in the permeability constants that in principle may be attached to individual cell types. These control the ease with which different cell species move through the barrier. In order to reduce the multiplication of entities for which there are, at present, only very limited independent data, we only specified permeability values for species moving in (K_{A_o}) or out (K_{A_i}) of the eye (a requirement imposed by considering the resting state of the system) and examined the impact of different values on movement in each direction. This was sufficient for the model to match the experimental data qualitatively. A 2.5-fold variation in K_{A_o} resulted in quite wide variation in the characteristic criteria of the model (Table 2). It was striking that values approaching experiment were achieved in situations where the permeability constant for cells moving out of the eye approached zero (but not if there was no movement). This raises the possibility that asymmetry in trafficking is critical to the accumulation of cells and its biological correlate might be the upregulation of chemokine/chemokine-receptor signals that retain cells within the eye. Interestingly, the model does not require that such cell trapping fluctuates for oscillations in cell numbers to occur, or for the model to approach the behaviour that we have demonstrated experimentally.

The model also provides insight into the importance of APC generation and homeostasis. Our results demonstrate

that the ratio of normal APC output to maximal APC output was a critical parameter that determined whether oscillation occurred. This value could be derived from the set of parameters used in the model. Remarkably, its value of 1.3 falls within the range for the same ratio measured by experiment in the 1970s (1.1–1.6) [22]. This focuses attention on the importance that the dynamics of APC generation and recruitment play in determining the magnitude and character of the inflammatory response. The complexity of the biology of this response far exceeds the scope of the model presented here [24–26], but our results underscore that it may drive as well as be driven by the antigen-specific adaptive response of T cells.

In summary we have studied a relatively simple model that neglects much of the biological complexity, including considerations such as compartment-dependent death rates and changes in cell-surface phenotype, that we understand regulate inflammation. By considering cell numbers on either side of a barrier as a function of cell concentration and permeability properties of the barrier, we have been able to produce results that are qualitatively in good agreement with experimental data, although of limited quantitative fidelity. We can conclude that the simplifying assumption, that cell traffic can be modelled by the application of the laws of mass action, is sufficient to produce a model that can mimic much of the behaviour demonstrated by experiment. Furthermore, the model draws attention to our need to understand better the permeability properties of the barrier from the perspective of the individual cell types, as well as suggesting that the dynamics of the process are dependent on the turnover and maximum rate of production of APCs.

Acknowledgments The authors would like to thank Heping Xu for unpublished data quantifying the volume of the mouse retina. This work was supported by the National Eye Research Centre.

Appendix: Details of the model

Our modelling approach is based on the principles of immune-response models that have been proposed and analysed in earlier literature. The model is expressed in terms of the customary mass action equations, where it is assumed that concentration heterogeneities are unimportant; a significant distinction from earlier models is that different concentrations can exist on opposite sides of the barrier. The possible dynamic processes are characterised by rate constants controlling production, proliferation, death (apoptosis for cells), activation or transformation (differentiation) of one species to another produced by contact with another species in the system, and permeation through the barrier.

One advantage of single-compartment models is that, being limited to only three or four cell populations, they lend themselves well to the analytical techniques of dynamical systems. With the introduction of a barrier and the consequent effects on the population dynamics, our model requires at least seven variables, and rigorous mathematical analysis becomes intractable. While there is a clear interest in keeping the number of model variables to a minimum, we have introduced a further three cell populations in order to represent important aspects of the cell dynamics. These are: the immunisation concentration of APCs that do not permeate the barrier; ‘mother’ and ‘daughter’ activated T-cell populations constructed to represent the proliferation/differentiation process during clonal expansion; and a population of memory T cells whose existence may be significant for the longer-term response. Investigations of a model that omits memory cells suggest that sustained oscillatory behaviour similar to that observed experimentally does not occur when T_o is maintained at the concentration level of about 5 cm^{-3} indicated by experimental data [27]. After an immune response, T cells that become memory cells increase the total concentration of antigen-specific T cells that can then be reactivated by activated APCs increases.

The basic mechanisms operating in our model are summarised as follows:

- Naïve T-cell numbers (T_o) in the resting state are maintained through a homeostatic combination of cell production, cell division and apoptosis. In contact with activated APCs, they become a first generation of ‘mother’ effector T cells (T_m^*). The unactivated T_o cells do not permeate the barrier [28].
- Mother effector T cells (T_m^*) either undergo apoptosis, or divide into N generations of daughter effector T cells (T_d^*). The mother effector T cells are not allowed to permeate the barrier—this restriction reflects the observation that activated T-cell proliferation inside the eye is inhibited by the local environment. In the circulation, activated T-cell division is not inhibited [14, 15]. Neglecting permeation of this population is justified by the relatively small proportion of mother cells to daughter cells.
- Daughter effector T cells are activated (T_d^*) and can permeate the barrier, undergo apoptosis, or differentiate into (unactivated) memory T cells. The population is bounded, due to spatial and nutritional factors.
- Memory T cells (T_M) can also be activated into mother cells (T_m^*), or undergo apoptosis. The memory T cells do not permeate the barrier. This population is also bounded due to spatial and nutritional factors.
- The immunisation population of APCs that initiate the immune response (A_{oo}) only undergoes apoptosis. It is

considered to be an immobilised population of APCs in the periphery (likely to be dendritic cells), and cannot permeate the barrier.

- APCs outside the retina (A_o) in the resting state are maintained through a homeostatic combination of cell production, cell division, apoptosis and permeation through the barrier.
- APCs inside the retina (A_i) in the resting state are maintained through a homeostatic combination of entry (permeation) through the barrier and apoptosis. They can acquire retinal antigen and be activated on contact with activated T cells, otherwise they undergo apoptosis.
- Activated APCs inside the retina (A_i^*) have acquired retinal antigen and can permeate through the barrier, or undergo apoptosis.
- Activated APCs outside the retina (A_o^*) can permeate the barrier, undergo apoptosis and activate naïve T cells.

The following set of equations defines the time evolution, during EAU, of the species listed in Table 2, according to the system described above. Each equation is constructed as the sum of components representing the basic mechanisms listed above.

$$\frac{dT_o}{dt} = a_T + p_T T_o \left(1 - \frac{T_o}{T_L}\right) - \delta_T T_o - \alpha_T T_o (A_o^* + A_{oo}^*) \quad (1)$$

$$\frac{dT_m^*}{dt} = -\delta_T^* T_m^* + \alpha_T (T_o + T_M) (A_o^* + A_{oo}^*) - H_1(t) p_T^* T_m^* \quad (2)$$

$$\frac{dT_M}{dt} = -\delta_T T_M + H_2(t) \beta T_d^* \left(1 - \frac{T_M}{T_{ML}}\right) - \alpha_T T_M (A_o^* + A_{oo}^*) \quad (3)$$

$$\begin{aligned} \frac{dT_d^*}{dt} = & -(K_{T_d}^* T_d^* - K_{T_i}^* T_i^*) f(T_i^*) h(t) \\ & + H_1(t) (N - 1) p_T^* T_m^* \left(1 - \frac{T_d^*}{T_{dL}}\right) \\ & - \delta_T^* T_d^* - H_2(t) \beta T_d^* \left(1 - \frac{T_M}{T_{ML}}\right) \end{aligned} \quad (4)$$

$$\frac{dT_i^*}{dt} = v (K_{T_d}^* T_d^* - K_{T_i}^* T_i^*) f(T_i^*) h(t) - \delta_T^* T_i^* \quad (5)$$

$$\begin{aligned} \frac{dA_o}{dt} = & a_A + p_A A_o \left(1 - \frac{A_o}{A_L}\right) - (K_{A_o} A_o - K_{A_i} A_i) f(T_i^*) h(t) \\ & - \delta_A A_o \end{aligned} \quad (6)$$

$$\frac{dA_i}{dt} = v (K_{A_o} A_o - K_{A_i} A_i) f(T_i^*) h(t) - \delta_A A_i - \alpha_A T_i^* A_i \quad (7)$$

$$\frac{dA_o^*}{dt} = -(K_{A_o}^* A_o^* - K_{A_i}^* A_i^*) f(T_i^*) h(t) - \delta_A^* A_o^* \quad (8)$$

$$\frac{dA_i^*}{dt} = v(K_{A_o}^* A_o^* - K_{A_i}^* A_i^*)f(T_i^*)h(t) - \delta_A^* A_i^* + \alpha_A T_i^* A_i \quad (9)$$

$$\frac{dA_{oo}^*}{dt} = -\delta_A^* A_{oo}^* \quad (10)$$

The following constants are used in the rate equations with appropriate subscripts/superscripts to denote the species to which they apply:

α , activation of $T_i \rightarrow T_i^*$ (α_T) or $A_i \rightarrow A_i^*$ (α_A); β , differentiation of activated (effector) daughter cells to memory cells; δ , apoptosis (cell death); K , permeability constant; a , production of T cells (a_T) or A cells (a_A); p , division of naïve T cells (p_T), proliferation of mother cells to daughter cells (p_T^*), and division of A_o cells (p_A); $f(T_i^*)$, permeation rate dependence on T_i^* (see below); $h(t)$, permeation rate dependence on time (see below); H_n , Heaviside switching functions ($H_n = 0$ below a time threshold and $H_n = 1$ above the threshold) that account for the delay in proliferation of daughter cells [29] ($n = 1$) and the time lag between cell recognition and cell division and differentiation [30] ($n = 2$); v , the ratio of the volume occupied by populations within the retina to the volume occupied by populations in the peripheral volume; T_L, T_{dL}, T_{ML} and A_L , limiting concentrations in the production and proliferation terms for the respective species in Eqs. (1), (3), (4) and (6). The general properties of the production and proliferation terms are discussed more fully below [Eq. (13)]; $(N-1)$, the maximum number of daughter cells generated by a mother cell.

For the remainder of this section, we examine some of the terms appearing in Eqs. (1)–(10) in further detail.

Barrier permeation

The permeation rate through the barrier is assumed to be proportional to the concentrations on either side of the barrier. The principle of mass balance underlying our equations requires the introduction of the factor v for permeation-related terms in the evolution equations for species inside the eye. The unperturbed barrier is permeable to activated cells, and the permeability increases with the concentration T_i^* up to a saturation limit [18]. We account for this by introducing a function $f(T_i^*)$ which modifies the barrier permeability in response to the increase in leukocyte concentration inside the eye:

$$f(T_i^*) = \frac{\mu + \sigma T_i^*}{\mu + T_i^*} \quad (11)$$

In Eq. (11), σ is a dimensionless constant and μ has the dimensions of concentration. $f(T_i^*)$ approaches the limit σ when $T_i^* \rightarrow \infty$, is unity when $T_i^* = 0$ and has the value $(1 + \sigma)/2$ when the concentration $T_i^* = \mu$. If T_i^* oscillates, then $f(T_i^*)$ also does so.

Permeability is also modified at barrier breakdown after about 10 days [19, 31]. Here we introduce a sigmoid function $h(t)$ having the form:

$$h(t) = \frac{(1 + \exp(bt_D))^{\gamma}}{(1 + \exp[-b(t - t_D)])^{\gamma}} \quad (12)$$

with $h(0) = 1$; $h(\infty) = [1 + \exp(bt_D)]^{\gamma} = \phi$. We use input values for t_D , the amplification of the permeability, and $\dot{h}(t_D)/\gamma$ to determine the parameters for $h(t)$: γ is found to be in the range [0.5, 1.5] and b is in the range [0.2, 0.5].

In the equations, provision has been made for each of the initial permeability rates to be different. This allows, for example, that the barrier may be asymmetrical, or that biological modifications to the cells on either side may alter their rate of transport. The model makes no allowance for spatial variations in cell concentration on either side of the membrane.

Homeostasis

In mice and humans, homeostasis in the populations of naïve T cells and APCs is maintained by replenishment from the thymus and bone marrow, respectively. To represent homeostatic processes for a concentration c we use logistic equations [16, 17] with a production rate a and proliferation (division) constant p :

$$\frac{dc}{dt} = a + pc \left(1 - \frac{c}{c_L}\right) \quad (13)$$

The merits of this and other possible forms have been discussed in several places [13, 16, 32], and we have chosen this approach as it is widely applied in related models. As pointed out by May [16], Eq. (13) suffers from the disadvantage that proliferation rates can become negative when $c > c_L$. We return to this point below. An alternative form for the homeostatic limitation of memory cells specifically has been proposed in which the population is controlled by Heaviside switching functions [12].

Species ‘transformation’: activation or proliferation

The product terms: $\alpha_A T_i^* A_i$ and $\alpha_T T_o(A_o^* + A_{oo}^*)$ represent the activation of APCs by activated T cells, and the activation of naïve T cells (into ‘mother’ activated T cells) by activated APCs, respectively. The proliferation process results in $(N - 1)$ daughter cells: however, this process is mediated by the availability of space and nutrition for activated cells. To reflect this upper bound in daughter numbers, we employ a logistic term. With similar justification, a logistic term is also included for the conversion of daughter cells into memory cells (in the outer compartment).

Parameters

Where suitable values could be found, we have used parameters estimated from data in the literature, or from our own experiments. Some of the parameters in the above equations were not available, or could only be estimated within orders of magnitude. This applies in particular to the permeability constants, and we have simplified these considerably by reducing their number to only two.

Some constraints on parameters emerge as a consequence of the resting behaviour predicted by the model. We investigated the effects of varying several of the parameters in order to explore the range of behaviour accessible to our set of equations.

Individual rate processes such as apoptosis, population growth by cell doubling, or permeation across the barrier, driven by a species concentration gradient, can be expressed in a general form $dc/dt = \pm kc(t)$ for a population concentration $c(t)$. In the absence of other effects, the resultant concentration evolves as $c = c(0)\exp(\pm kt)$. Thus we can estimate rate constants from the rate at which these individual processes double or halve a population.

Concentrations are expressed in number of cells per mL (cm^{-3}). There are approximately 10^7 white blood cells in the murine circulation [33, 34]; of these approximately 5 % are monocytes, which we identify with A_o in our equations, equivalent to a resting state concentration of $5 \times 10^5 \text{ cm}^{-3}$. The resting state concentration of naïve T cells (T_o) specific for a unique determinant, at about 5 cm^{-3} , is very much lower [27]. The resting state concentration of A cells inside the eye (A_i) is $2.9 \times 10^5 \text{ cm}^{-3}$, based on experimental cell counts [3] and a mouse eye retinal volume of $2.29 \times 10^{-3} \text{ cm}^3$ (H. Xu, personal communication).

The doubling time for activated T cells has been estimated to be between 8 and 12 h [12, 30]. The naïve T cell population replenishes itself at a rather slower rate of less than once per day [35]. The division and maintenance of a stable population, which is the major factor in maintaining T-cell homeostasis [36], has recently been considered in detail [37].

The half-life for naïve T cells is quite long [37], while that of activated T cells has been estimated as between 2 and 6 days [30, 38]. The dendritic cells that initiate the immune response (A_{oo}^*) and do not pass the BRB have an estimated half-life of 3 days [30, 39].

Activation of T (α_T) cells by dendritic cells has been given as $10^{-3} \text{ cm}^3 \text{ day}^{-1}$ [30] as an ad hoc parameter. The subsequent process of differentiation of effector cells to memory cells has been widely discussed [40–44] and several models have been proposed recently [42, 44–46]. In some models CD8^+ rather than CD4^+ cells have been modelled; however, Kallies [43] has argued that

comparable dynamics apply to both types. Our equations correspond most closely to the linear differentiation model discussed (with others) by Ganusov [44]. Data fitting from the publications cited suggest a half-life of between 600 and 900 h for the differentiation process.

The maximum increase in the barrier permeability due to T_i^* [σ in Eq. (11)] is of the order of 10^3 [18]. Calculations are not very sensitive to the other parameter in this equation, μ , which was set at $1,000 \text{ cm}^{-3}$. We choose a similar order of magnitude for the increase in permeability due to barrier disruption ($\phi = 500$) from Eq. (12).

In the next section we deduce values for the permeability constant and show that a_T , the rate of production of naïve T cells from the thymus per unit volume, and a_A , the rate of production of A_o cells from the bone marrow, are bounded by the model.

Equilibrium

Equations (1)–(10) define the evolution in a phase space of accessible states for which the resting state represents the equilibrium state in the absence of disease. The only non-zero concentrations in this state are T_o^c , the concentration of naïve T cells in the resting state, and A_o^c and A_i^c , the resting-state concentrations of the (unactivated) APCs outside and inside the retina, respectively. As the resting state is an equilibrium point, T_o^c is given by the equation

$$\frac{2p_T}{T_L} T_o^c = (p_T - \delta_T) + \left[(p_T - \delta_T)^2 + \frac{4p_T a_T}{T_L} \right]^{1/2} \quad (15)$$

Equation (15) can be re-arranged as an expression for T_L , the limiting concentration that will sustain this concentration in the absence of any other perturbation:

$$\frac{T_L}{T_o^c} = \frac{p_T T_o^c}{a_T + (p_T - \delta_T) T_o^c} \quad (16)$$

We define $q = T_L/T_o^c$, and impose the constraint $q > 1$: this ensures that the cell division term (p_T) in Eq. (1) is positive in the resting state, where a negative rate of T-cell division would not have any biological meaning. This does not of course imply that dT_o/dt cannot be negative; this can occur if the rate of cell death is high enough.

A further consequence of the constraint $q > 1$ is that the rate of cell production $a_T \leq \delta_T T_o^c$, since the numerator in Eq. (16) must be greater than the denominator, which therefore sets an upper bound for a_T . Estimates for the parameters show that the half-life for naïve T cells is much longer than the doubling time for production and consequently that $p_T > \delta_T$. Using the doubling time and half-life from Table 3, $p_T = 2.9 \times 10^{-2} \text{ h}^{-1}$ and $\delta_T = 5.07 \times 10^{-4} \text{ h}^{-1}$. q has an approximately linear dependence on a_T , with a maximum value of $q = p_T/(p_T - \delta_T) = 1.018$ and a

minimum value of 1.0 (when $a_T = \delta_T T_0^c \approx 2.5 \times 10^{-3} \text{ h cm}^{-3}$).

The maintenance of homeostasis according to the logistic equation therefore imposes an upper bound on the rate of cell production from the thymus. With suitable parameter and time-step choices, and in the absence of other influences, the analytical and numerical solutions of Eq. (15) return a constant value of T_0^c with time.

The only other species present in the resting state are A_o and A_i ; the rates of change of their concentrations in this state (when the factors modifying the permeability are unity) are given by

$$\frac{dA_o}{dt} = a_A + p_A A_o \left(1 - \frac{A_o}{A_L}\right) - (K_{A_o} A_o - K_{A_i} A_i) - \delta_A A_o \tag{17}$$

$$\frac{dA_i}{dt} = v(K_{A_o} A_o - K_{A_i} A_i) - \delta_A A_i \tag{18}$$

The steady-state values A_o^c and A_i^c , determined by the zeroes of Eqs. (17) and (18), can be expressed in terms of the ratio $\theta = A_L/A_o^c$ [in analogy to the definition of q in Eq. (16)]

$$\theta = \frac{A_L}{A_o^c} = \frac{A_o^c p_A}{a_A - A_o^c B} \tag{19}$$

in which B is defined by the expression

$$B = -p_A + \delta_A + K_{A_o} \delta_A / (vK_{A_i} + \delta_A) \tag{20}$$

and the ratio of A_i^c and A_o^c determined from Eq. (18):

$$\frac{A_i^c}{A_o^c} = A = \frac{vK_{A_o}}{vK_{A_i} + \delta_A} \tag{21}$$

Equation (21) shows that the equilibrium populations of APCs inside and outside the retina are not equal if the barrier permeability is the same in each direction. If we choose a single permeability constant $K_A = K_{A_o} = K_{A_i}$, then Eq. (21) shows that $A_o^c > A_i^c$, as supported by experimental observation.

Equation (19) can be rearranged as an expression for a_A

$$a_A = A_o^c \left[\frac{B\theta + p_A}{\theta} \right] \tag{22}$$

As for T_o , we note from its definition that if $\theta < 1$, the rate of production of APCs [the second term in Eq. (17)] would be negative at equilibrium (i.e. $A_o^c/A_L > 1$), which does not have any meaning, and therefore θ cannot be less than unity.

Substitution of Eq. (21) into Eq. (20) gives

$$B = -p_A + \delta_A + A\delta_A/v \tag{23}$$

which, with Eq. (22), yields an expression for the rate of production of A cells:

$$a_A = A_o^c \left[\delta_A(1 + A/v) - \frac{p_A(\theta - 1)}{\theta} \right] \tag{24}$$

Since $a_A > 0$, Eq. (24), leads to an upper limit for θ :

$$\theta < \frac{1}{[1 - \delta_A(1 + A/v)]/p_A} \tag{25}$$

In most calculations we have used the ratio of retinal to vascular volumes of 61.9 (Xu, personal communication) as an estimate for v . The estimated values for δ_A and p_A (Table 1) give an upper limit of 1.313 for θ when v is given a value of 61.9. We have remarked that the peripheral volume is uncertain and may be larger, in which case v would be smaller than 61.9. Equation (25) sets a lower limit on v of 0.180, since θ_{max} then becomes < 0 , but increases to a large positive value close to this limit. The maximum value permissible for the peripheral volume on this basis is $12.7 \times 10^{-3} \text{ cm}^3$. Equation (24) yields the fractional turnover rate of A_o cells of approximately 1/100 every hour. Calculations show the value of θ has to be very close to its maximum value for oscillations to occur; typically, if θ/θ_{max} is below ~ 0.995 , the system does not oscillate. This upper limit on θ restricts the production limit A_L in Eq. (6) and consequently the number of A_o cells that can be generated in this way.

From Eq. (21) we can make a first-order estimate for the permeability constants by assuming that they are identical and equal to K (say). Using the concentrations in Table 1, with $v = 61.9$ and $\delta_A = 9.627 \times 10^{-3} \text{ h}^{-1}$ from the half-life of 3 days in Table 3, yields $K = 2.14 \times 10^{-4} \text{ h}^{-1}$. K_{A_i} can be calculated from Eq. (21) using this as an order of magnitude estimate for K_{A_o} . Since $K_{A_i} > 0$, Eq. (21) requires that $K_{A_o} > A\delta_A/v$ ($= 9.02 \times 10^{-5} \text{ h}^{-1}$ with the above parameter estimates) which sets a lower limit for K_{A_o} . An upper limit depends on several parameters which may themselves have a range of possible values. Trial calculations showed that this upper limit is approximately $2.6 \times 10^{-4} \text{ h}^{-1}$, and that the calculations could not be completed with higher permeabilities.

The single-compartment model

The single-compartment model is created by removing the barrier, and summing the pairs of Eqs. (4) + (5), (6) + (7) and (8) + (9). There is now no distinction between external and internal species, although mother, daughter, memory and naïve T cells remain distinct. The resulting single compartment model is expressed by:

$$\frac{dT^*}{dt} = H_1(N - 1)p_T^* T_m^* \left(1 - \frac{T_d^*}{T_{dL}}\right) - \delta_T^* T^* - H_2 \beta T_d^* \tag{26}$$

$$\frac{dA}{dt} = a_A + p_{AA} \left(1 - \frac{A}{A_L} \right) - \delta_A A - \alpha_A T_1^* A \quad (27)$$

$$\frac{dA^*}{dt} = -\delta_A^* A^* + \alpha_A T_1^* A \quad (28)$$

together with Eqs. (1), (2), (3) and (10) which are unchanged.

Stability of the resting state

The resting state is one of several fixed points in the system. The stability of the system with respect to this state is determined from the eigenvalues of the Jacobian of the time evolution operator. Analysis of the eigenvalues shows that the system is unstable with respect to the resting state when activated species are present. This differs from some existing single-compartment models, including those closely related to the single-compartment reduction of our model, whose resting state can demonstrate stability for sufficiently small perturbations [47].

References

- Kuchroo VK, Anderson AC, Waldner H, Munder M, Bettelli E, Nicholson LB. T cell response in experimental autoimmune encephalomyelitis (EAE): role of self and cross-reactive antigens in shaping, tuning, and regulating the autopathogenic T cell repertoire. *Annu Rev Immunol.* 2002;20(1):101–23.
- Xu H, Forrester JV, Liversidge J, Crane IJ. Leukocyte trafficking in experimental autoimmune uveitis: breakdown of blood-retinal barrier and upregulation of cellular adhesion molecules. *Invest Ophthalmol Vis Sci.* 2003;44(1):226–34.
- Kerr EC, Raveney BJE, Copland DA, Dick AD, Nicholson LB. Analysis of retinal cellular infiltrate in experimental autoimmune uveoretinitis reveals multiple regulatory cell populations. *J Autoimmun.* 2008;31:354–61.
- Raveney BJE, Copland DA, Nicholson LB, Dick AD. Fingolimod (FTY720) as an acute rescue therapy for intraocular inflammatory disease. *Arch Ophthalmol.* 2008;126:1390–5.
- Shao H, Shi H, Kaplan HJ, Sun D. Chronic recurrent autoimmune uveitis with progressive photoreceptor damage induced in rats by transfer of IRBP-specific T cells. *J Neuroimmunol.* 2005;163(1–2):102–9.
- Trudeau JD, Kelly-Smith C, Verchere CB, Elliott JF, Dutz JP, Finegood DT, Santamaria P, Tan R. Prediction of spontaneous autoimmune diabetes in NOD mice by quantification of autoreactive T cells in peripheral blood. *J Clin Invest.* 2003;111(2):217–23.
- Butcher EC, Picker LJ. Lymphocyte homing and homeostasis. *Science.* 1996;272(5258):60–7.
- Bradley LM. Migration and T-lymphocyte effector function. *Curr Opin Immunol.* 2003;15(3):343–8.
- Ley K, Laudanna C, Cybulsky MI, Nourshargh S. Getting to the site of inflammation: the leukocyte adhesion cascade updated. *Nat Rev Immunol.* 2007;7(9):678–89.
- Wodarz D, Nowak MA. Mathematical models of HIV pathogenesis and treatment. *BioEssays.* 2002;24(12):1178–87.
- Perelson AS. Modelling viral and immune system dynamics. *Nat Rev Immunol.* 2002;2(1):28–36.
- Antia R, Ganusov VV, Ahmed R. The role of models in understanding CD8+ T-cell memory. *Nat Rev Immunol.* 2005;5:101–11.
- Iwami S, Takeuchi Y, Miura Y, Sasaki T, Kajiwara T. Dynamical properties of autoimmune disease models: tolerance, flare-up, dormancy. *J Theor Biol.* 2007;246(4):646–59.
- Raveney BJE, Copland DA, Calder CJ, Dick AD, Nicholson LB. TNFR1 signalling is a critical checkpoint for developing macrophages that control of T-cell proliferation. *Immunology.* 2010;131:340–9.
- Raveney BJE, Copland DA, Dick AD, Nicholson LB. TNFR1-dependent regulation of myeloid cell function in experimental autoimmune uveoretinitis. *J Immunol.* 2009;183:2321–9.
- May RM. Biological populations with nonoverlapping generations: stable points, stable cycles, and chaos. *Science.* 1974;186(4164):645–7.
- Perelson AS, Nelson PW. Mathematical analysis of HIV-1 dynamics in vivo. *Siam Rev.* 1999;41(1):3–44.
- Jung U, Norman KE, Scharffetter-Kochanek K, Beaudet AL, Ley K. Transit time of leukocytes rolling through venules controls cytokine-induced inflammatory cell recruitment in vivo. *J Clin Invest.* 1998;102(8):1526–33.
- Luna JD, Chan CC, Derevjaniuk NL, et al. Blood-retinal barrier (BRB) breakdown in experimental autoimmune uveoretinitis: comparison with vascular endothelial growth factor, tumor necrosis factor alpha, and interleukin-1 beta-mediated breakdown. *J Neurosci Res.* 1997;49(3):268–80.
- Prendergast RA, Iliff CE, Coskuncan NM, Caspi RR, Sartani G, Tarrant TK, Luty GA, McLeod DS. T cell traffic and the inflammatory response in experimental autoimmune uveoretinitis. *Invest Ophthalmol Vis Sci.* 1998;39(5):754–62.
- Caspi RR. A look at autoimmunity and inflammation in the eye. *J Clin Invest.* 2010;120(9):3073–83.
- Van Furth R, Diesselhoff-den Dulk MC, Mattie H. Quantitative study on the production and kinetics of mononuclear phagocytes during an acute inflammatory reaction. *J Exp Med.* 1973;138(6):1314–30.
- Pedra JHF, Cassel SL, Sutterwala FS. Sensing pathogens and danger signals by the inflammasome. *Curr Opin Immunol.* 2009;21(1):10–6.
- Liu K, Victora GD, Schwickert TA, et al. In vivo analysis of dendritic cell development and homeostasis. *Science.* 2009;324(5925):392–7.
- Auffray C, Sieweke MH, Geissmann F. Blood monocytes: development, heterogeneity, and relationship with dendritic cells. *Annu Rev Immunol.* 2009;27(1):669–92.
- Kamei M, Carman CV. New observations on the trafficking and diapedesis of monocytes. *Curr Opin Hematol.* 2010;17(1):43–52.
- Moon JJ, Chu HH, Pepper M, McSorley SJ, Jameson SC, Kedl RM, Jenkins MK. Naive CD4+ T cell frequency varies for different epitopes and predicts repertoire diversity and response magnitude. *Immunity.* 2007;27(2):203–13.
- Pittet MJ, Mempel TR. Regulation of T-cell migration and effector functions: insights from in vivo imaging studies. *Immunol Rev.* 2008;221:107–29.
- Carreno LJ, Bueno SM, Bull P, Nathenson SG, Kalergis AM. The half-life of the T-cell receptor/peptide-major histocompatibility complex interaction can modulate T-cell activation in response to bacterial challenge. *Immunology.* 2007;121(2):227–37.
- Ludewig B, Krebs P, Junt T, Metters H, Ford NJ, Anderson RM, Bocharov G. Determining control parameters for dendritic cell-cytotoxic T lymphocyte interaction. *Eur J Immunol.* 2004;34(9):2407–18.

31. Kerr EC, Copland DA, Dick AD, Nicholson LB. The dynamics of leukocyte infiltration in experimental autoimmune uveoretinitis. *Prog Retin Eye Res.* 2008;27:527–35.
32. Perelson AS, Weisbuch G. Immunology for physicists. *Rev Mod Phys.* 1997;69(4):1219–67.
33. Everds NE. Hematology of the laboratory mouse. In: Fox J, Barthold S, Davisson M, Newcomer C, Quimby F, Smith A, editors. *The mouse in biomedical research Vol. III.* London: Academic Press; 2006. pp 133–170.
34. Rugh R, Somogyi C. The effect of pregnancy on peripheral blood in the mouse. *Biol Bull.* 1969;136(3):454–60.
35. De Boer RJ, Perelson AS. Towards a general function describing T cell proliferation. *J Theor Biol.* 1995;175(4):567–76.
36. Baev DV, Peng X-H, Song L, Barnhart JR, Crooks GM, Weinberg KI, Metelitsa LS. Distinct homeostatic requirements of CD4+ and CD4- subsets of Valpha24-invariant natural killer T cells in humans. *Blood.* 2004;104(13):4150–6.
37. Murray JM, Kaufmann GR, Hodgkin PD, Lewin SR, Kelleher AD, Davenport MP, Zaunders JJ. Naive T cells are maintained by thymic output in early ages but by proliferation without phenotypic change after age twenty. *Immunol Cell Biol.* 2003; 81(6):487–95.
38. Ruedl C, Koebel P, Bachmann M, Hess M, Karjalainen K. Anatomical origin of dendritic cells determines their life span in peripheral lymph nodes. *J Immunol.* 2000;165(9):4910–6.
39. Kamath AT, Pooley J, O’Keeffe MA, et al. The development, maturation, and turnover rate of mouse spleen dendritic cell populations. *J Immunol.* 2000;165(12):6762–70.
40. Geginat J, Sallusto F, Lanzavecchia A. Cytokine-driven proliferation and differentiation of human naive, central memory, and effector memory CD4(+) T cells. *J Exp Med.* 2001;194(12): 1711–9.
41. Manjunath N, Shankar P, Wan J, et al. Effector differentiation is not prerequisite for generation of memory cytotoxic T lymphocytes. *J Clin Invest.* 2001;108(6):871–8.
42. Reiner SL, Sallusto F, Lanzavecchia A. Division of labor with a workforce of one: challenges in specifying effector and memory T cell fate. *Science.* 2007;317(5838):622–5.
43. Kallies A. Distinct regulation of effector and memory T-cell differentiation. *Immunol Cell Biol.* 2008;86(4):325–32.
44. Ganusov VV. Discriminating between different pathways of memory CD8+ T cell differentiation. *J Immunol.* 2007;179(8): 5006–13.
45. Zand MS, Briggs BJ, Bose A, Vo T. Discrete event modeling of CD4+ memory T cell generation. *J Immunol.* 2004;173(6): 3763–72.
46. Kohler B. Mathematically modeling dynamics of T cell responses: predictions concerning the generation of memory cells. *J Theor Biol.* 2007;245(4):669–76.
47. De Leenheer P, Smith HL. Virus dynamics: a global analysis. *Siam J Appl Math.* 2003;63:1313–27.
48. Antia R, Bergstrom CT, Pilyugin SS, Kaech SM, Ahmed R. Models of CD8+ responses: 1. What is the antigen-independent proliferation program. *J Theor Biol.* 2003;221(4):585–98.
49. Zhou GM, Strom RC, Giguere V, Williams RW. Modulation of retinal cell populations and eye size in retinoic acid receptor knockout mice. *Mol Vision.* 2001;7(36):253–60.
50. Jecker P, Pabst R, Westermann J. Proliferating macrophages, dendritic cells, natural killer cells, T and B lymphocytes in the middle ear and Eustachian tube mucosa during experimental acute otitis media in the rat. *Clin Exp Immunol.* 2001;126(3): 421–5.